DOI: 10.1002/ejoc.201200339

Modular Solid-Phase Synthesis of Teroxazoles as a Class of α-Helix Mimetics

Cristiano Pinto Gomes,[a][‡] Alexander Metz,[b][‡] Jan W. Bats,[a] Holger Gohlke,[b] and Michael W. Göbel*[a]

Keywords: Protein–protein interactions / Conformation analysis / Molecular dynamics / Peptidomimetics / Helical structures

α-Helices are ubiquitous structural elements of proteins and are important in molecular recognition. Small molecules mimicking α-helices have proven to be valuable biophysical probes or modulators of protein-protein interactions. Here, we present modeling studies and the modular solid-phase synthesis of teroxazole derivatives as a new class of α-helix mimetics. The synthesis is compatible with a variety of functional groups and should thus be generally applicable for generating diversely substituted oligo-oxazole scaffolds. The teroxazole scaffold is predicted to be polar and to project peptidomimetic side chains at positions *i*, *i*+3, and *i*+6 of an α-helix, which complements projection patterns of existing helix mimetics. The scaffold retains sufficient conformational flexibility to conform to induced-fit models of protein-protein interaction inhibition.

Introduction

α-Helices are ubiquitous structural elements of proteins and are important in molecular recognition.[1] Accordingly, small molecules mimicking α-helices have proven to be valuable biophysical probes or modulators of protein-protein interactions (PPI).[2] Typically, only some of the side chains of an α-helix form interaction "hot spots" in PPI.[3] Imitating these interactions by using α-helix mimetics thus offers a route to the rational development of PPI modulators.[4]

Initial approaches to mimic α-helices with non-peptidic compounds began more than two decades ago.[2a,2c,5] Small α-helix mimetics, such as derivatives of allenes, alkylidene cycloalkanes, spiranes, biphenyls,[6] bicyclic indanes,[7] and benzodiazepinediones[8] often mimic α-helix positions that are at close range. A pioneering achievement was the design and synthesis of terphenyl derivatives (Scheme 1, **I**) by the Hamilton group.[9] Such extended scaffolds are substituted with R groups that mimic the position and orientation of C_α–C_β launch vectors of side chains on one "face" of an α-helix. Terphenyl derivatives have been shown to inhibit Bak/Bcl-X_L[10] and p53/HDM2[11] interactions at submicromolar concentrations.[9,12] However, terphenyls are rather hydrophobic, which led to the development of other scaffolds that are more hydrophilic and/or amphiphilic including oligopyridines,[13] phenylpyridals,[14] phenylenaminones,[15] benzoylureas,[16] oxazole-pyridazine-piperazines (Scheme 1, **II**) and oxazole-pyrrole-piperazines,[17] 1,4-dipiperazino benzenes,[18] 5-6-5 imidazole-phenyl-thiazoles, terphthalimides,[19] biphenyl 4,4′-dicarboxamides,[20] oligobenzamides,[21] and 6/6/6/6 *trans*-fused polycyclic ethers.[22]

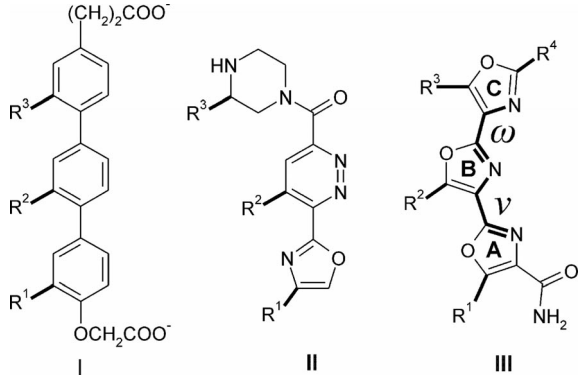

Scheme 1. Terphenyl (**I**), oxazole-pyridazine-piperazine (**II**), and teroxazole (**III**) scaffolds for α-helix mimicry. R^1–R^4 = CH_3 or peptidomimetic side chain. The inter-ring torsion angles, *v* and *ω*, of **III** are highlighted in bold. Oxazole rings of **III** are labeled **A**, **B**, and **C**.

Here, we describe molecular modeling studies and the modular solid-phase synthesis of teroxazole derivatives (Scheme 1, **III**)[23] as a new class of α-helix mimetics. The modeling studies suggest that substituted teroxazoles are hydrophilic and preferentially project R groups with launch vectors similar to those of side chains at positions *i*, *i*+3,

[a] Institute of Organic Chemistry and Chemical Biology, Department of Biochemistry, Chemistry, and Pharmacy, Goethe-University,
Max-von-Laue-Str. 7, 60438 Frankfurt, Germany
Fax: +49-69-798-29464
E-mail: m.goebel@chemie.uni-frankfurt.de
[b] Institute for Pharmaceutical and Medicinal Chemistry, Department of Mathematics and Natural Sciences, Heinrich-Heine-University,
Universitätsstr. 1, 40225 Düsseldorf, Germany
[‡] Both authors contributed equally to this work.
Supporting information for this article is available on the WWW under http://dx.doi.org/10.1002/ejoc.201200339.

and *i*+6 of an α-helix. This suggestion was confirmed by single-crystal structures. This projection pattern complements that of previous scaffolds and covers a broader region on the α-helix surface, which may be advantageous when it comes to mimicking interactions between two helices that wrap around each other and/or are not arranged in a collinear way.

Results and Discussion

Modeling Studies

Computation of relative molecular mechanics Poisson–Boltzmann surface area (MM-PB/SA)[24] effective energies as a function of inter-ring torsion angles v and ω reveal that teroxazoles can adopt low-energy conformations with an α-helix-like arrangement of side chains (Scheme 1, **III**; Figure 1a). The conformation with both torsion angles eclipsed (v = 0°, ω = 0°) has the lowest energy. Rotating one or both of the torsion angles by 180° increases the effective energy by approximately 2 and 4 kcal mol^{-1}, respectively. The prevalence of the (v = 0°, ω = 0°) conformation can be explained by a parallel orientation of the ring dipoles leading to a more favorable solvation contribution (data not shown). The rotation around v or ω is hindered by an energy barrier of ≈5.5 kcal mol^{-1}, but nonetheless occurs multiple times during a molecular dynamics (MD) simulation of 250 ns length (Figure 2). The torsion angle distributions from the MD trajectory also reveal significant deviations of v and ω of up to 50° from a coplanar orientation of the rings. This observation is in good agreement with the MM-PB/SA computations that yield an energetic cost of ≈3 kcal mol^{-1} for such a deviation. The apparent torsional flexibility is expected to enable the teroxazole scaffold to project peptidomimetic side chains fulfilling distance and angular requirements of an α-helix, and to conform to induced-fit models of protein-protein interaction inhibition.[15]

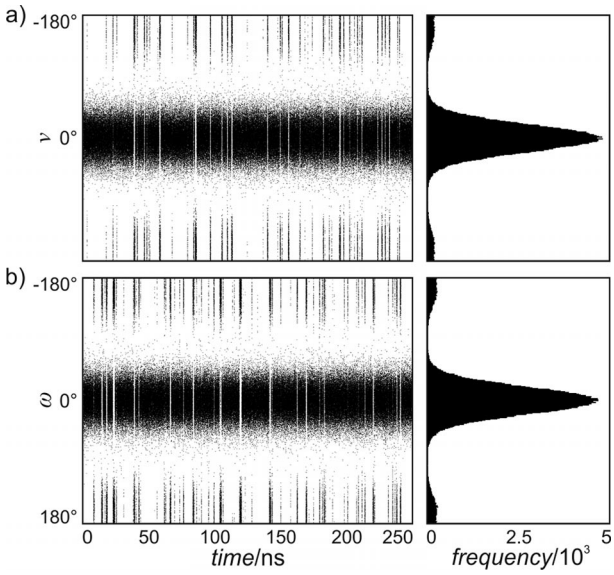

Figure 2. Mutual orientation of teroxazole rings in aqueous solution. The inter-ring torsion angles, v and ω, of **13a** in explicit solvent were calculated from a MD trajectory of 250 ns length at intervals of 1 ns. Depicted are the inter-ring torsion angles (a) v and (b) ω as a function of the simulation time (left panels) and in terms of histograms (right panels) with bins of 1°. The inter-ring torsion angles are defined in Scheme 1, **III**.

Superimposing the substituents R^1–R^4 of coplanar teroxazole conformations onto C$_\beta$ atoms of a canonical α-helical octapeptide reveals that the teroxazole scaffold can

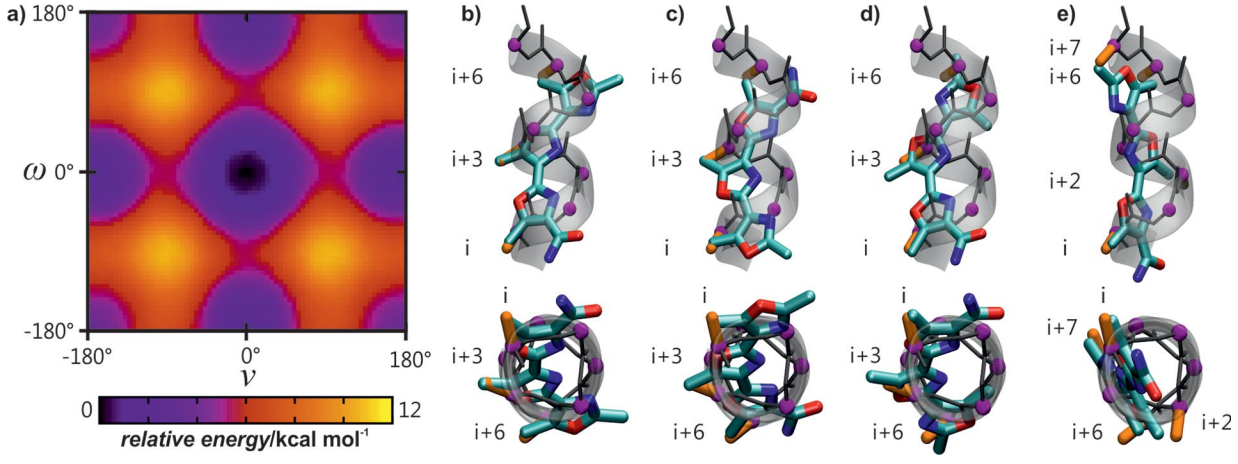

Figure 1. Preferred conformation of a teroxazole scaffold in aqueous solution. (a) Relative MM-PB/SA[36] effective energies of teroxazole **13a** as a function of the inter-ring torsion angles v and ω (Scheme 1, **III**). (b) Superimposition of C$_\beta$ atoms of side chains at positions *i*, *i*+3, and *i*+6 of a canonical α-helical octapeptide onto the corresponding substituent atoms of R$^{1–3}$ of a teroxazole in a low-energy conformation (v = 0°, ω = 0°). (c) Analogous alignments with the teroxazole scaffold reversed with respect to the α-helix axis. (d) Making use of the substituent R^4 of a rotated ring C (v = 0°, ω = 180°). (e) If ring A is rotated instead (v = 180°, ω = 0°), it is possible to align all four substituents R$^{1–4}$ with α-helix side chains at positions *i*, *i*+2, *i*+6, and *i*+7. Below, the α-helix/α-helix-mimetics superimpositions were rotated by 90°. The N-terminus of the α-helix is oriented towards the viewer. The relative MM-PB/SA effective energies of the conformations of **13a** used for (b) or (c), (d), and (e) are 0.30, 2.48 and 1.96 kcal mol^{-1}, respectively. Graphics by gnuplot[39] and VMD.[40]

closely mimic the arrangement of peptide side chains (Figure 1b–e). Good agreement is found for the minimum energy conformation (v = 0°, ω = 0°) with ring A pointing towards the N-terminus of the α-helix, mimicking α-helix positions *i*, *i*+3, and *i*+6 [root mean square deviation (RMSD) = 0.35 Å; Figure 1b]. Reversing the orientation of the teroxazole scaffold with respect to the α-helix axis does not change the positional agreement between substituent atoms and C_β atoms but impairs the orientational agreement between the respective bonds (Figure 1c). Rotating ring C by 180° (v = 0°, ω = 180°; Figure 1d) allows the substituent at R^4 to be used. In this conformation the distance between the substituents in ring A or B and ring C is increased, which results in a poorer superimposition with respect to C_β atoms (RMSD = 1.03 Å). Because R^3 and R^4 are located on opposite edges of ring C, it is not possible to align them to amino-acid side chains located on one "face" of an α-helix. Nevertheless, in situations where the mimicked α-helix is deeply buried, one could imagine making use of all four substituents arranged as side chains in positions *i*, *i*+2, *i*+6, and *i*+7 (RMSD = 0.84 Å, Figure 1e). The side chains now form two pairs [(*i*, *i*+7) and (*i*+2, *i*+6)], each of which is located on one "face" of an α-helix. Alternatively, if substituent R^3 or R^4 is not required to mimic an important interaction site, it can be used to fine-tune physicochemical and pharmacokinetic properties.

Terphenyl[10–12] and oxazole-pyridazine-piperazine[17] derivatives mimic side chain positions *i*, *i*+3/i+4, and *i*+7. In both cases, the side chains are located on one "face" of an α-helix. On the contrary, the side chain positions *i*, *i*+3, and *i*+6 addressed by coplanar teroxazole derivatives cover a broader region on the α-helix surface that is rarely addressed by other α-helix mimetics.[25] This broader region may be advantageous to mimic interactions between two helices that wrap around each other and/or are not arranged in a collinear way. α-Helix mimetics based on terphenyl scaffolds are rather hydrophobic (Scheme 1, **I** with R^1–R^4 = CH_3; log *P* = 3.34) that may compromise the water solubility and, hence, the biocompatibility. Among others[13,19] oxazole-pyridazine-piperazine scaffolds[17a] have been developed as more polar alternatives to enhance solubility (Scheme 1, **II** with R^1–R^4 = CH_3; log *P* = 0.96). Likewise, the teroxazole scaffold introduced here is polar and should offer increased solubility (Scheme 1, **III** with R^1–R^4 = CH_3: log *P* = 0.34). These modeling studies suggest teroxazoles as a new class of α-helix mimetics, the R-groups of which point in the directions of side chains of the α-helix that are preferentially located on one face of the helix.

Chemistry

We envisioned a fast and reliable procedure to prepare substituted teroxazoles starting from easily available precursors. Owing to the fact that naturally occurring oligo-oxazoles bearing a C2–C4 linkage pattern are derived from serine containing substrates,[26] substituents at C5 can be obtained from functionalized β-hydroxy-α-amino acids. Starting from these precursors, construction of a peptide followed by further oxazole building transformations is expected to result in the desired heterocycles (Scheme 2).

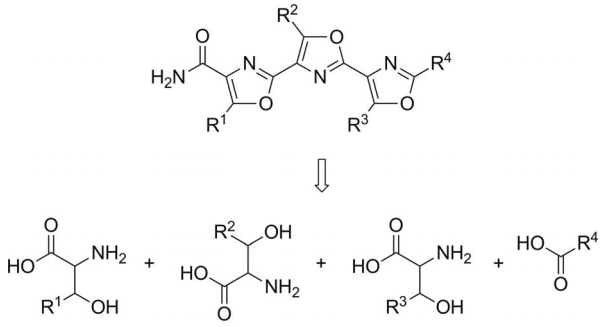

Scheme 2. Retrosynthetic disconnection of the teroxazole scaffold.

Wipf and Miller,[27] showed that β-hydroxy amides can be efficiently converted to C5-substituted oxazole subunits. The reaction conditions are very mild and therefore compatible with a variety of functional groups [e.g., amides, esters, 9*H*-fluoren-9-ylmethoxycarbonyl (Fmoc), Boc, Alloc, and Cbz]. Kessler et al.[28] extended this concept by applying it to solid-phase synthesis to offer a valuable tool for the rapid construction of highly-substituted oxazole moieties. Based on these findings we developed a general solid-phase strategy for the preparation of a teroxazole scaffold. This procedure allows incorporation of structurally different side chains into the framework employing a modular concept. Moreover, the method should be appropriate for use in parallel synthesis. The retrosynthetic approach is shown in Scheme 2. The strategy includes incorporation of four components to introduce structural diversity. Substituted β-hydroxy-α-amino acids and a simple carboxylic acid are required as building blocks for the synthesis. These monomers can be readily connected by using standard amide bond-forming reactions [1-hydroxybenzotriazole (HOBt)/diisopropylcarbodiimide (DIC)], allowing rapid and efficient access to peptidic precursors for further transformations. We chose a solid-phase approach that benefits from the facile purification and reaction work-up owing to the immobilized substrate. The key step involves a modified Gabriel–Robinson cyclization of the peptidic precursor.[27] The required β-ketoamide is generated by oxidation of the side chain alcohol and subsequently converted into the oxazole by cyclodehydration. Repeating the cycle of peptide coupling, oxidation, and cyclodehydration led to the desired teroxazole compounds.

Synthesis of the Building Blocks

The building blocks were prepared by aldol addition of protected glycine derivative **1**[29] and corresponding aldehydes to yield β-hydroxy-α-amino acid *tert*-butyl esters **2** as racemic mixtures of diastereomers (Scheme 3). At this stage both diastereomers could be separated by column chromatography for analytical purposes. However, because the newly generated stereocenters are lost in the oxidation-

cyclodehydration sequence to form the resin-bound oxazole moiety, there is no need for a stereoselective aldol reaction or a separation of stereoisomers. Subsequent cleavage of the *tert*-butyl esters under strongly acidic conditions afforded the hydrochloride salt of the amino acids that were subsequently protected resulting in **3**. Finally, the secondary hydroxy groups were converted into the trityl ethers in the presence of in situ generated trityl triflate[30,31] to provide the orthogonally protected β-hydroxy-α-amino acids **4**.

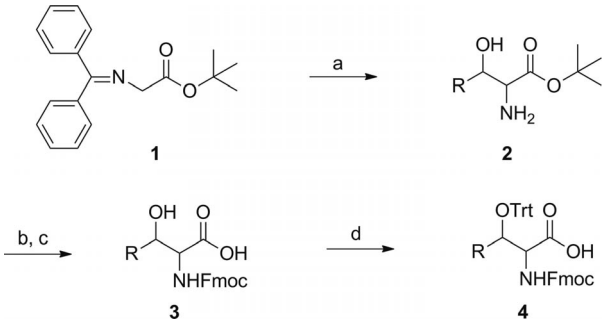

Scheme 3. General synthesis of orthogonally protected β-hydroxy-α-amino acids bearing nonpolar residues: (a) (i) 1 M Lithium hexamethyldisilazide (LHMDS), THF, –78 °C; (ii) RCHO, THF, –78 °C; (iii) 1 M HCl, THF, 0 °C. (b) 6 M HCl, reflux. (c) *N*-(9*H*-Fluoren-9-ylmethoxycarbonyloxy)succinimide, Na_2CO_3, 1,4-dioxane/water (1.2:1), 0 °C to room temp. (d) TrtCl, AgOTf, 2,6-lutidine, CH_2Cl_2, 0 °C to room temp. (**2a**: R = CH_2CH_2NHCbz; **2b** and **3b**: R = Et; **2c**, **3c**, and **4**: R = *i*Bu; **2d** and **3d**: R = CH_2-1-naphthyl)

Solid-Phase Synthesis of Teroxazole Derivatives

The synthesis was performed on Rink amide 4-methylbenzhydrylamine hydrochloride salt (MBHA) resin (**5**) at a scale of 0.25 mmol by using standard solid-phase techniques and Fmoc/triphenylmethyl (Trt) synthetic procedures (Scheme 4). The resin-bound Fmoc group was removed with piperidine in dimethylformamide (DMF; 20%, v/v), followed by attachment of Fmoc-protected β-hydroxy-α-amino acids **3** to the solid support in the presence of HOBt/DIC. Treatment of the resin with piperidine and coupling of Fmoc/Trt-protected β-hydroxy-α-amino acids **4** with HOBt/DIC formed the immobilized dipeptides **6**. The corresponding β-ketoamides **7** were obtained by oxidation of the hydroxy group with Dess–Martin periodinane (DMP). Subsequent treatment of the ketone with PPh_3/I_2 afforded oxazole derivatives **8** by a Robinson–Gabriel cyclodehydration.[27] Cleavage of the trityl ether with 1% trifluoroacetic acid (TFA) in dichloromethane in the presence of a scavenger and removal of the Fmoc group with piperidine were followed by coupling of **4** with HOBt/DIC to provide resin-bound β-hydroxyamides **9**. After oxidation to the β-ketoamide with Dess–Martin periodinane, cyclodehydration with PPh_3/I_2 resulted in resin-bound bioxazole derivatives **10**. Removal of the Fmoc protecting group with piperidine was followed by coupling of the terminal carboxylic acid (HOBt/DIC). After cleavage of the trityl ether with diluted TFA, peptides **11** were subjected to oxidation and cyclodehydration as before. Resin-bound teroxazole derivatives **12** were finally cleaved from the support under acidic conditions and purified by column chromatography affording **13**.

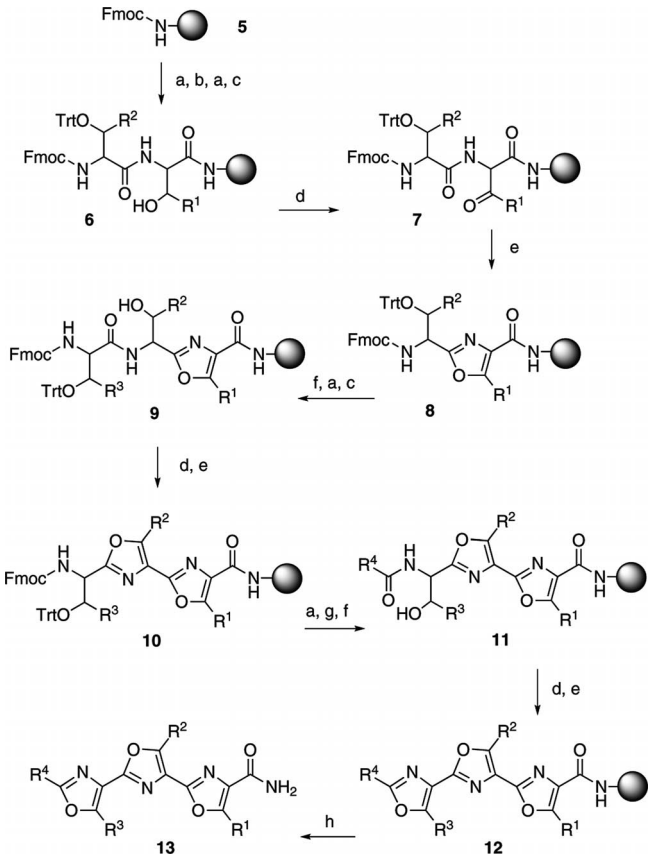

Scheme 4. Solid-phase synthesis of the teroxazole scaffold: (a) Piperidine/DMF (1:4). (b) Fmoc-protected amino acid **3**, HOBt, DIC, NMP. (c) Fmoc/Trt-protected amino acid **4**, HOBt, DIC, NMP. (d) Dess–Martin periodinane, CH_2Cl_2. (e) PPh_3, I_2, DIPEA, CH_2Cl_2. (f) TFA/TIPS/CH_2Cl_2 (1:5:94). (g) Carboxylic acid, HOBt, DIC, NMP or acetic anhydride, DIPEA, NMP. (h) TFA/TIPS/H_2O (95:2.5:2.5). (**13a**: R^1–R^4 = Me; **13b**: R^1 = Et, R^2 = *i*Bu, R^3 = Me, R^4 = Bn; **13c**: R^1–R^3 = *i*Bu)

Applying this methodology, teroxazole derivatives **13a**–**c** (Scheme 5) were synthesized starting from protected β-hydroxy-α-amino acids in overall yields of 19–24%, corresponding to average yields per step above 90%. Solid-phase syntheses are normally conducted on a small scale providing only small quantities of target compounds. However, **13a**–**c** could be obtained in quantities of around 20 mg, sufficient for most scientific purposes (0.25 mmol of resin-bound NH_2).

We also synthesized a set of monooxazoles bearing different types of side chains and functional groups to demonstrate the structural diversity accessible by our method (Scheme 6). The products obtained comprise alkyl, aryl, basic, and acidic residues.

To obtain the precursors of **14f** and **14g**, we had to modify some reaction conditions and protecting groups (Scheme 7). In the case of **14f** it was necessary to use milder

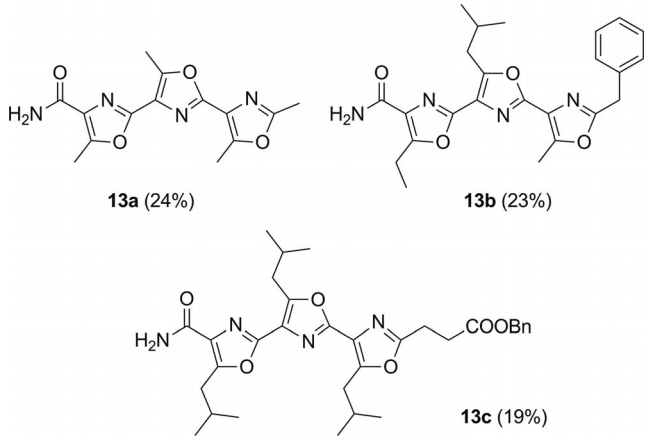

Scheme 5. Teroxazole derivatives **13a**–**c** synthesized in this study.

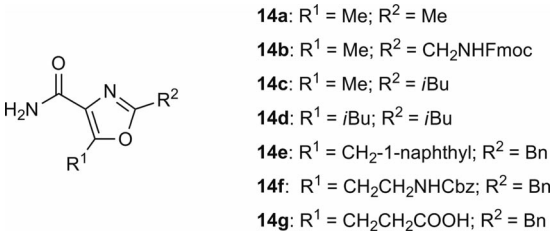

Scheme 6. Structures of the substituted monooxazoles **14a**–**g**.

conditions for the cleavage of the *tert*-butyl ester **2a** to prevent premature loss of the Cbz group. The deprotection was achieved with a mixture of TFA/CH_2Cl_2 (1:1) at room temperature affording **15**. The *tert*-butyl ester of O'Donnell imine **1** needed to be replaced during the preparation of **14g** because the carboxyl group at the side chain of the aldehyde already contained this protecting group. When benzyl ester **16** was used in the aldol reaction yielding **17**, subsequent hydrogenolysis at atmospheric pressure removed the benzyl group furnishing free β-hydroxy-α-amino acid **18** that was further protected as shown in Scheme 3.

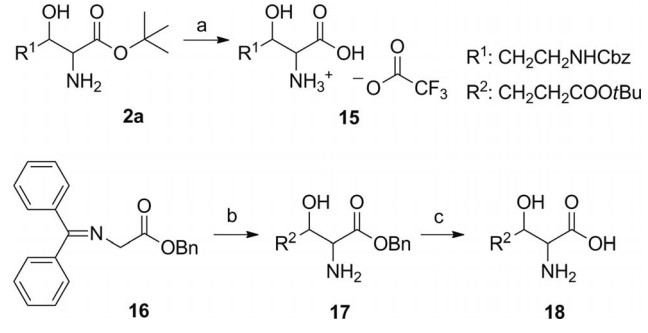

Scheme 7. Modified preparation of unprotected β-hydroxy-α-amino acids: (a) TFA/CH_2Cl_2 (1:1), room temp. (b) (i) 1 M LHMDS, THF, –78 °C; (ii) R^2CHO, THF, –78 °C; (iii) 1 M HCl, THF, 0 °C. (c) H_2, Pd/C, 1 bar, room temp.

Single crystals of **13a** and **13b** suitable for X-ray crystallographic analysis were obtained by slow solvent evaporation (ethyl acetate). These structures confirm the coplanar orientation of the oxazole rings found to be energetically favorable in the modeling studies, with *v*/*ω* values of 178.6/179.4° and 6.9/–6.1° for **13a** and **13b**, respectively (Figure 3).

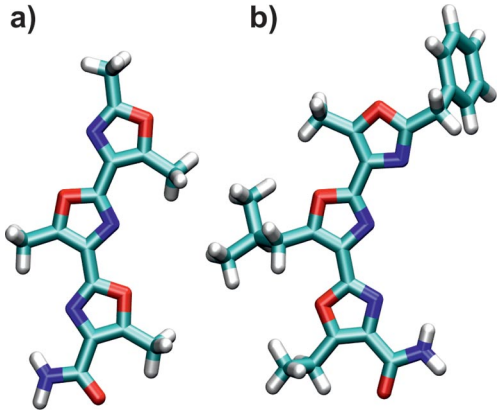

Figure 3. Single-crystal structures of (a) **13a** and (b) **13b**.

Conclusions

A modular solid-phase synthesis of a series of α-helix mimetics based on a teroxazole scaffold is presented. The synthesis starts from substituted β-hydroxy-α-amino acids, is compatible with a variety of functional groups, and should thus be applicable for generating diversely substituted oligo-oxazole scaffolds. Molecular modeling studies demonstrate that teroxazoles are able to mimic the side chains *i*, *i*+3, and *i*+6 of an α-helix, which cover a broader region on the α-helix surface than peptidomimetic side chains presented by terphenyl or oxazole-pyridazine-piperazine scaffolds. Furthermore, the teroxazole scaffold is found to be more hydrophilic than the terphenyl scaffold and as hydrophilic as the oxazole-pyridazine-piperazine scaffold, which should result in improved solubility and biocompatibility. At present, a series of teroxazoles synthesized with the methods presented above is being evaluated for its potential to act as protein-protein interaction modulators.

Experimental Section

Conformational and Physicochemical Properties: The inter-ring torsion angles *v* and *ω* (Scheme 1, scaffold **III** and Figure 1a) are crucial for the conformational properties of the teroxazole scaffold. Hence, the respective torsion angle potential was parameterized for use with other parameters of the molecular mechanics general AMBER force field (GAFF).[32] Conformations of the bioxazole derivative 2′,5,5′-trimethyl-[2,4′-bioxazole]-4-carboxamide (**28**, see Supporting Information) were optimized at the MP2/6-31G* level by using Gaussian 03,[33] with the inter-ring torsion angles *υ* and *ω* constrained at intervals of 15° over a range of 360°. Likewise, the conformations were optimized – constrained to the same inter-ring torsion angles – by using the GAFF force field within

AMBER 9.[34] Torsion potential energies for each torsion angle position were obtained by subtracting the GAFF molecular mechanics energy, devoid of the contribution of the inter-ring torsion, from the MP2/6-31G* energy of the corresponding optimized structures. A new molecular mechanics torsion angle potential was then determined by fitting the appropriate GAFF term to these torsion potential energies. This torsion angle potential was used for both inter-ring torsions v and ω of teroxazole **13a** (Figure 1a with $R^{1–4} = CH_3$) in the calculations below. Partial charges for the bi- and teroxazoles were derived by multiconformational RESP fitting[35] to the HF/6-31G* electrostatic potentials of the optimized conformations with coplanar rings.

To determine the conformational preferences of **13a**, relative MM-PB/SA[36] effective energies were calculated for conformations that had been optimized by using the GAFF force field with the inter-ring torsion angles constrained at intervals of 5° over a range of 360° (Figure 1b). Next, minimization, equilibration, and MD simulations of **13a** in explicit solvent was carried out with the AMBER 9 program package by using the GAFF force field and standard procedures (TIP3P water model, PBC, PME, SHAKE, time step of 2 ps). The distribution of torsion angles was analyzed over a MD trajectory of 250 ns length (Figure 2).

log P values of α-helix mimetics in Scheme 1 were calculated by Molinspiration MiLog P,[37] which has been shown to have good predictive power (root mean square error = 1.10) in a recent study on a dataset of ≈96000 compounds.[38]

General Procedures for Solid-Phase Reactions

Coupling of Carboxylic Acids or Protected Amino Acids: A solution of the corresponding carboxylic acid or protected amino acid (3 equiv.), HOBt·H_2O (3 equiv.) and DIC (3 equiv.) in *N*-methyl-2-pyrrolidone (NMP; 3 mL) was stirred (10 min) at room temperature and added to the resin-bound amine. The suspension was agitated until the reaction was complete (monitored by the Kaiser test). The resin was washed with NMP (5×).

Acylation with Anhydrides: A mixture of the corresponding anhydride (2 × 5 equiv.) and *N*,*N*-diisopropylethylamine (DIPEA; 2 × 5 equiv.) in NMP (5 mL) was added to the resin-bound amine and agitated (2 × 30 min) at room temperature. After the reaction was complete (monitored by the Kaiser test) the resin was washed with NMP (5×).

Removal of Fmoc Protecting Groups: The resin-bound Fmoc-protected amine was treated with 20% piperidine in DMF (1 × 5 min, 1 × 20 min, 1 × 10 min) and washed with NMP (5×).

Removal of Triphenylmethyl Protecting Groups: A mixture of TFA/triisopropylsilane (TIPS)/CH_2Cl_2 (1:5:94) was added to the resin-bound Trt-protected alcohol, agitated (2 × 10 min, 3 × 5 min) at room temperature and washed with CH_2Cl_2 (5×).

Cleavage from the Resin: The resin-bound oxazole derivative was treated with a mixture of TFA/TIPS/H_2O (95:2.5:2.5) at room temperature (2 h). After washing the solid support with CH_2Cl_2 (3×), the filtrate and washings were combined and concentrated in vacuo.

Preparation of Teroxazoles

Typical Procedure: 2′′-Benzyl-5-ethyl-5′-isobutyl-5′′-methyl-[2,4′:2′,4′′-teroxazole]-4-carboxamide (13b): Rink amide MBHA resin (391 mg, 0.25 mmol, 0.64 mmol/g loading) was swelled in NMP (1 h), followed by removal of the Fmoc protecting group. After coupling of amino acid **3b** (R = ethyl, mixture of isomers, 267 mg, 0.75 mmol), the Fmoc protecting group was removed and compound **4** (R = isobutyl, mixture of isomers, 469 mg, 0.75 mmol) was coupled to the resin. Washing with CH_2Cl_2 (5×) was followed by treatment (2 h) of the resin with DMP (0.1 M, 7.5 mL, 0.75 mmol) in CH_2Cl_2. The resin was washed with CH_2Cl_2 (5×), NMP (5×) and CH_2Cl_2 (5×), and a solution of PPh_3 (656 mg, 2.50 mmol), iodine (635 mg, 2.50 mmol) and DIPEA (871 μL, 5.00 mmol) in CH_2Cl_2 (17 mL) was added. After shaking (12 h), the Trt protecting group was cleaved, and the resin was washed with NMP (5×). The Fmoc protecting group was removed and Fmoc-*O*-trityl-L-threonine (438 mg, 0.75 mmol) was coupled to the resin-bound amine. The resin was washed with CH_2Cl_2 (5×), treated (2 h) with a solution of DMP (0.1 M, 7.5 mL, 0.75 mmol) in CH_2Cl_2 and washed with CH_2Cl_2 (5×), NMP (5×) and CH_2Cl_2 (5×). A solution of PPh_3 (656 mg, 2.50 mmol), iodine (635 mg, 2.50 mmol) and DIPEA (871 μL, 5.00 mmol) in CH_2Cl_2 (17 mL) was added and agitated (12 h), followed by washing with CH_2Cl_2 (5×) and NMP (5×). After removal of the Fmoc protecting group, phenylacetic acid (102 mg, 0.75 mmol) was attached to the resin-bound amine. The resin was washed with CH_2Cl_2 (5×), the trityl protecting group was removed and a solution of DMP (0.1 M, 7.5 mL, 0.75 mmol) in CH_2Cl_2 was added. The suspension was agitated (2 h), washed with CH_2Cl_2 (5×), NMP (5×) and CH_2Cl_2 (5×) and treated (12 h) with a solution of PPh_3 (656 mg, 2.50 mmol), iodine (635 mg, 2.50 mmol) and DIPEA (871 μL, 5.00 mmol) in CH_2Cl_2 (17 mL). The resin was washed with CH_2Cl_2 (5×), NMP (5×) and CH_2Cl_2 (5×), followed by cleavage of the resin. The brown residue was purified by column chromatography (silica gel; *n*-hexane/ethyl acetate, 1:1) and recrystallized (cyclohexane), providing **13b** (25 mg, 23%) as a colorless solid. M.p. 185–187 °C. R_f = 0.52 (ethyl acetate/*n*-hexane, 9:1). IR (KBr): $\tilde{\nu}$ = 3471 (m), 3350 (w), 3276 (w), 3131 (m), 2957 (m), 2871 (w), 1689 (s), 1649 (m), 1628 (m), 1586 (m), 1551 (w), 1496 (w), 1455 (m), 1419 (m), 1386 (w), 1368 (w), 1350 (w), 1248 (w), 1198 (m), 1161 (w), 1096 (w), 1064 (s), 1034 (s), 985 (w), 946 (w), 801 (w), 773 (w), 729 (m), 696 (m), 669 (w), 567 (w) cm^{-1}. ^1H NMR (250 MHz, $CDCl_3$): δ = 0.94 [d, J = 6.7 Hz, 6 H, $(CH_3)_2CH$], 1.27 (t, J = 7.6 Hz, 3 H, CH_3CH_2), 2.13 [m, 1 H, $(CH_3)_2CH$], 2.61 (s, 3 H, ArCH_3), 2.95 (d, J = 7.2 Hz, 2 H, *i*PrCH_2), 3.12 (q, J = 7.6 Hz, 2 H, CH_2CH_3), 4.08 (s, 2 H, CH_2Ph), 5.43 (br. s, 1 H, NH_2), 6.85 (br. s, 1 H, NH_2), 7.17–7.30 (m, 5 H, C_6H_5) ppm. ^{13}C NMR (101 MHz, $CDCl_3$): δ = 11.8, 12.1, 19.4, 22.4, 28.3, 34.5, 34.5, 124.7, 126.1, 127.2, 128.7, 128.7, 128.8, 135.0, 150.8, 153.1, 153.1, 155.3, 158.2, 161.8, 163.8 ppm. $C_{24}H_{26}N_4O_4$ (434.49): calcd. C 66.34, H 6.03, N 12.89; found C 66.11, H 5.95, N 12.88.

2′′,5,5′,5′′-Tetramethyl-[2,4′:2′,4′′-teroxazole]-4-carboxamide (13a): Monomers used: Fmoc-L-threonine, Fmoc-*O*-trityl-L-threonine and acetic anhydride. The reaction gave **13a** as colorless solid (24%). M.p. 254–255 °C from ethyl acetate/*n*-hexane. R_f = 0.12 (ethyl acetate/*n*-hexane, 9:1). IR (KBr): $\tilde{\nu}$ = 3455 (m), 3338 (w), 3272 (w), 3190 (m), 2929 (w), 1674 (s), 1648 (m), 1634 (w), 1622 (m), 1592 (m), 1575 (w), 1552 (m), 1429 (m), 1372 (w), 1334 (m), 1307 (w), 1291 (w), 1244 (m), 1206 (m), 1180 (w), 1122 (m), 1053 (s), 983 (m), 945 (w), 936 (w), 799 (w), 768 (w), 745 (w), 735 (w), 696 (w), 680 (m), 630 (w) cm^{-1}. ^1H NMR (250 MHz, $CDCl_3$): δ = 2.48 (s, 3 H, CH_3), 2.69 (s, 3 H, CH_3), 2.72 (s, 3 H, CH_3), 2.73 (s, 3 H, CH_3), 5.91 (br. s, 1 H, NH_2), 6.97 (br. s, 1 H, NH_2) ppm. ^{13}C NMR (63 MHz, $CDCl_3$): δ = 11.67, 11.69, 11.8, 13.7, 124.2, 125.4, 129.1, 149.9, 150.2, 153.3, 154.1, 155.0, 160.5, 165.0 ppm. $C_{14}H_{14}N_4O_4$ (302.29): calcd. C 55.63, H 4.67, N 18.53; found C 55.71, H 4.78, N 18.25.

Benzyl 3-(4′′-Carbamoyl-5,5′,5′′-triisobutyl-[2′,4:2′′,4′-teroxazole]-2-yl)propanoate (13c): Monomers used: Fmoc-protected β-hydroxy-α-amino acid **3c** (R = isobutyl, mixture of isomers), Fmoc/Trt-protected β-hydroxy-α-amino acid **4** (R = isobutyl, mixture of isomers)

and monobenzyl succinate (**23**). The reaction gave **13c** as a colorless semi-solid (19%). R_f = 0.42 (*n*-hexane/ethyl acetate, 1:1). IR (KBr): $\tilde{\nu}$ = 3471 (m), 3353 (w), 3279 (w), 3142 (w), 2958 (s), 2926 (m), 2870 (m), 1734 (s), 1686 (s), 1647 (w), 1624 (m), 1588 (m), 1546 (w), 1466 (m), 1430 (w), 1387 (w), 1368 (w), 1340 (w), 1196 (w), 1166 (m), 1095 (w), 1031 (m), 801 (w), 792 (w), 751 (w), 698 (m), 645 (w), 582 (w), 512 (m) cm^{-1}. ^1H NMR (400 MHz, $CDCl_3$): δ = 0.96 [d, J = 6.7 Hz, 6 H, $(CH_3)_2CH$], 0.99 [d, J = 6.5 Hz, 6 H, $(CH_3)_2CH$], 1.00 [d, J = 6.5 Hz, 6 H, $(CH_3)_2CH$], 2.03–2.22 [m, 3 H, $(CH_3)_2CH$], 2.92 (t, J = 7.6 Hz, 2 H, CH_2CH_2), 2.94 (d, J = 7.2 Hz, 2 H, *i*PrCH_2), 3.00 (d, J = 7.1 Hz, 2 H, *i*PrCH_2), 3.04 (d, J = 7.1 Hz, 2 H, *i*PrCH_2), 3.14 (t, J = 7.4 Hz, 2 H, CH_2CH_2), 5.14 (s, 2 H, CH_2Ph), 5.65 (br. s, 1 H, NH_2), 6.95 (br. s, 1 H, NH_2), 7.28–7.40 (m, 5 H, Ph) ppm. ^{13}C NMR (101 MHz, $CDCl_3$): δ = 22.29, 22.30, 22.4, 23.4, 28.06, 28.07, 28.3, 31.0, 34.3, 34.4, 34.5, 66.6, 125.1, 126.1, 128.2, 128.3, 128.5, 129.9, 135.7, 152.9, 153.2, 153.6, 155.3, 156.5, 162.0, 163.8, 171.6 ppm. HRMS (MALDI): calcd. for $C_{32}H_{40}N_4O_6+H^+$ [M + H$^+$] 577.3021; found 577.3020.

CCDC-866342 (for **13a**) and -866343 (for **13b**) contain the supplementary crystallographic data for this paper. These data can be obtained free of charge from The Cambridge Crystallographic Data Centre via www.ccdc.cam.ac.uk/data_request/cif.

Supporting Information (see footnote on the first page of this article): Synthetic procedures, characterization data for all new compounds, ^1H and ^{13}C NMR spectra and the crystal structure of bioxazole **28**.

Acknowledgments

Financial support by the Förderfonds der Goethe-Universität is gratefully acknowledged. H.G. is grateful to the Zentrum für Informations- und Medientechnologie of the Heinrich-Heine-University, Düsseldorf, for computational support and to the Strategischer Forschungsfond of the Heinrich-Heine-University, Düsseldorf, for financial support.

[1] a) M. P. H. Stumpf, T. Thorne, E. de Silva, R. Stewart, H. J. An, M. Lappe, C. Wiuf, *Proc. Natl. Acad. Sci. USA* **2008**, *105*, 6959–6964; b) A. G. Cochran, *Curr. Opin. Chem. Biol.* **2001**, *5*, 654–659.

[2] a) J. M. Davis, L. K. Tsou, A. D. Hamilton, *Chem. Soc. Rev.* **2007**, *36*, 326–334; b) M. R. Arkin, M. Randal, W. L. DeLano, J. Hyde, T. N. Luong, J. D. Oslob, D. R. Raphael, L. Taylor, J. Wang, R. S. McDowell, J. A. Wells, A. C. Braisted, *Proc. Natl. Acad. Sci. USA* **2003**, *100*, 1603–1608; c) J. A. Wells, C. L. McClendon, *Nature* **2007**, *450*, 1001–1009.

[3] a) T. Clackson, J. A. Wells, *Science* **1995**, *267*, 383–386; b) M. J. Ramos, I. S. Moreira, P. A. Fernandes, *Proteins Struct., Funct., Bioinf.* **2007**, *68*, 803–812; c) R. Nussinov, Z. J. Hu, B. Y. Ma, H. Wolfson, *Proteins Struct., Funct., Genet.* **2000**, *39*, 331–342; d) A. A. Bogan, K. S. Thorn, *J. Mol. Biol.* **1998**, *280*, 1–9; e) R. Nussinov, S. E. A. Ozbabacan, A. Gursoy, O. Keskin, *Curr. Opin. Drug Discovery Dev.* **2010**, *13*, 527–537; f) A. Metz, C. Pfleger, H. Kopitz, S. Pfeiffer-Marek, K.-H. Baringhaus, H. Gohlke, *J. Chem. Inf. Comput. Sci.* **2012**, *52*, 120–133.

[4] D. Gonzalez-Ruiz, H. Gohlke, *Curr. Med. Chem.* **2006**, *13*, 2607–2625.

[5] a) M. W. Peczuh, A. D. Hamilton, *Chem. Rev.* **2000**, *100*, 2479–2493; b) E. Ko, J. Liu, K. Burgess, *Chem. Soc. Rev.* **2011**, *40*, 4411–4421; c) E. Ko, J. Liu, L. M. Perez, G. L. Lu, A. Schaefer, K. Burgess, *J. Am. Chem. Soc.* **2011**, *133*, 462–477.

[6] E. Jacoby, *Bioorg. Med. Chem. Lett.* **2002**, *12*, 891–893.

[7] D. C. Horwell, W. Howson, G. S. Ratcliffe, H. M. G. Willems, *Bioorg. Med. Chem.* **1996**, *4*, 33–42.

[8] B. L. Grasberger, T. B. Lu, C. Schubert, D. J. Parks, T. E. Carver, H. K. Koblish, M. D. Cummings, L. V. LaFrance, K. L. Milkiewicz, R. R. Calvo, D. Maguire, J. Lattanze, C. F. Franks, S. Y. Zhao, K. Ramachandren, G. R. Bylebyl, M. Zhang, C. L. Manthey, E. C. Petrella, M. W. Pantoliano, I. C. Deckman, J. C. Spurlino, A. C. Maroney, B. E. Tomczuk, C. J. Molloy, R. F. Bone, *J. Med. Chem.* **2005**, *48*, 909–912.

[9] J. T. Ernst, O. Kutzki, A. K. Debnath, S. Jiang, H. Lu, A. D. Hamilton, *Angew. Chem.* **2002**, *114*, 288–291; *Angew. Chem. Int. Ed.* **2002**, *41*, 278–281.

[10] a) H. Yin, G. I. Lee, K. A. Sedey, O. Kutzki, H. S. Park, B. P. Omer, J. T. Ernst, H. G. Wang, S. M. Sebti, A. D. Hamilton, *J. Am. Chem. Soc.* **2005**, *127*, 10191–10196; b) O. Kutzki, H. S. Park, J. T. Ernst, B. P. Orner, H. Yin, A. D. Hamilton, *J. Am. Chem. Soc.* **2002**, *124*, 11838–11839.

[11] H. Yin, G. I. Lee, H. S. Park, G. A. Payne, J. M. Rodriguez, S. M. Sebti, A. D. Hamilton, *Angew. Chem.* **2005**, *117*, 2764–2767; *Angew. Chem. Int. Ed.* **2005**, *44*, 2704–2707.

[12] B. P. Orner, J. T. Ernst, A. D. Hamilton, *J. Am. Chem. Soc.* **2001**, *123*, 5382–5383.

[13] J. M. Davis, A. Truong, A. D. Hamilton, *Org. Lett.* **2005**, *7*, 5405–5408.

[14] G. T. Bourne, D. J. Kuster, G. R. Marshall, *Chem. Eur. J.* **2010**, *16*, 8439–8445.

[15] M. J. Adler, A. D. Hamilton, *J. Org. Chem.* **2011**, *76*, 7040–7047.

[16] a) J. M. Rodriguez, N. T. Ross, W. P. Katt, D. Dhar, G. I. Lee, A. D. Hamilton, *ChemMedChem* **2009**, *4*, 649–656; b) J. M. Rodriguez, A. D. Hamilton, *Angew. Chem.* **2007**, *119*, 8768–8771; *Angew. Chem. Int. Ed.* **2007**, *46*, 8614–8617.

[17] a) L. Moisan, S. Odermatt, N. Gombosuren, A. Carella, J. Rebek, *Eur. J. Org. Chem.* **2008**, 1673–1676; b) S. M. Biros, L. Moisan, E. Mann, A. Carella, D. Zhai, J. C. Reed, J. Rebek, *Bioorg. Med. Chem. Lett.* **2007**, *17*, 4641–4645.

[18] P. Maity, B. König, *Org. Lett.* **2008**, *10*, 1473–1476.

[19] H. Yin, A. D. Hamilton, *Bioorg. Med. Chem. Lett.* **2004**, *14*, 1375–1379.

[20] J. M. Rodriguez, L. Nevola, N. T. Ross, G. I. Lee, A. D. Hamilton, *ChemBioChem* **2009**, *10*, 829–833.

[21] I. Saraogi, C. D. Incarvito, A. D. Hamilton, *Angew. Chem.* **2008**, *120*, 9837–9840; *Angew. Chem. Int. Ed.* **2008**, *47*, 9691–9694.

[22] H. Oguri, S. Tanabe, A. Oomura, M. Umetsu, M. Hirama, *Tetrahedron Lett.* **2006**, *47*, 5801–5805.

[23] C. Pinto Gomes, Diploma Thesis, Goethe-University Frankfurt (D), **2007**.

[24] a) H. Gohlke, D. A. Case, *J. Comput. Chem.* **2004**, *25*, 238–250; b) H. Gohlke, C. Kiel, D. A. Case, *J. Mol. Biol.* **2003**, *330*, 891–913; c) J. Srinivasan, T. E. Cheatham, P. Cieplak, P. A. Kollman, D. A. Case, *J. Am. Chem. Soc.* **1998**, *120*, 9401–9409; d) P. A. Kollman, I. Massova, C. Reyes, B. Kuhn, S. H. Huo, L. Chong, M. Lee, T. Lee, Y. Duan, W. Wang, O. Donini, P. Cieplak, J. Srinivasan, D. A. Case, T. E. Cheatham, *Acc. Chem. Res.* **2000**, *33*, 889–897; e) N. Homeyer, H. Gohlke, *Mol. Informatics* **2012**, *31*, 114–122.

[25] a) J. S. Albert, M. S. Goodman, A. D. Hamilton, *J. Am. Chem. Soc.* **1995**, *117*, 1143–1144; b) J. S. Albert, M. W. Peczuh, A. D. Hamilton, *Bioorg. Med. Chem.* **1997**, *5*, 1455–1467.

[26] R. S. Roy, A. M. Gehring, J. C. Milne, P. J. Belshaw, C. T. Walsh, *Nat. Prod. Rep.* **1999**, *16*, 249–263.

[27] P. Wipf, C. P. Miller, *J. Org. Chem.* **1993**, *58*, 3604–3606.

[28] E. Biron, J. Chatterjee, H. Kessler, *Org. Lett.* **2006**, *8*, 2417–2420.

[29] M. J. O'Donnell, R. L. Polt, *J. Org. Chem.* **1982**, *47*, 2663–2666.

[30] R. M. Burk, T. S. Gac, M. B. Roof, *Tetrahedron Lett.* **1994**, *35*, 8111–8112.

[31] J. T. Lundquist IV, A. D. Satterfield, J. C. Pelletier, *Org. Lett.* **2006**, *8*, 3915–3918.

[32] J. M. Wang, R. M. Wolf, J. W. Caldwell, P. A. Kollman, D. A. Case, *J. Comput. Chem.* **2004**, *25*, 1157–1174.
[33] M. J. Frisch, G. W. Trucks, H. B. Schlegel, G. E. Scuseria, M. A. Robb, J. R. Cheeseman, J. J. A. Montgomery, T. Vreven, K. N. Kudin, J. C. Burant, J. M. Millam, S. S. Iyengar, J. Tomasi, V. Barone, B. Mennucci, M. Cossi, G. Scalmani, N. Rega, G. A. Petersson, H. Nakatsuji, M. Hada, M. Ehara, K. Toyota, R. Fukuda, J. Hasegawa, M. Ishida, T. Nakajima, Y. Honda, O. Kitao, H. Nakai, M. Klene, X. Li, J. E. Knox, H. P. Hratchian, J. B. Cross, V. Bakken, C. Adamo, J. Jaramillo, R. Gomperts, R. E. Stratmann, O. Yazyev, A. J. Austin, R. Cammi, C. Pomelli, J. W. Ochterski, P. Y. Ayala, K. Morokuma, G. A. Voth, P. Salvador, J. J. Dannenberg, V. G. Zakrzewski, S. Dapprich, A. D. Daniels, M. C. Strain, O. Farkas, D. K. Malick, A. D. Rabuck, K. Raghavachari, J. B. Foresman, J. V. Ortiz, Q. Cui, A. G. Baboul, S. Clifford, J. Cioslowski, B. B. Stefanov, G. Liu, A. Liashenko, P. Piskorz, I. Komaromi, R. L. Martin, D. J. Fox, T. Keith, M. A. Al-Laham, C. Y. Peng, A. Nanayakkara, M. Challacombe, P. M. W. Gill, B. Johnson, W. Chen, M. W. Wong, C. Gonzalez, J. A. Pople, *Gaussian 03*, Gaussian, Inc., Wallingford, CT, **2004**.
[34] D. A. Case, T. E. Cheatham, T. Darden, H. Gohlke, R. Luo, K. M. Merz, A. Onufriev, C. Simmerling, B. Wang, R. J. Woods, *J. Comput. Chem.* **2005**, *26*, 1668–1688.
[35] P. Cieplak, W. D. Cornell, C. Bayly, P. A. Kollman, *J. Comput. Chem.* **1995**, *16*, 1357–1377.
[36] I. Massova, P. A. Kollman, *Perspect. Drug Discovery Des.* **2000**, *18*, 113–135.
[37] Molinspiration Cheminformatics "Molinspiration" to be found under http://www.molinspiration.com/cgi-bin/properties **2008**.
[38] a) R. Mannhold, G. I. Poda, C. Ostermann, I. V. Tetko, *J. Pharm. Sci.* **2009**, *98*, 861–893; b) R. Mannhold, G. I. Poda, C. Ostermann, I. V. Tetko, *Chem. Biodiversity* **2009**, *6*, 1837–1844.
[39] T. Williams, C. Kelley, gnuplot 4.2, *Vol. 4.2*, **2009**.
[40] W. Humphrey, A. Dalke, K. Schulten, *J. Mol. Graphics* **1996**, *14*, 33–38.

Received: February 13, 2012
Published Online: May 8, 2012

